NACA

E51E07

RESEARCH MEMORANDUM

SOME EFFECTS OF SOLIDITY ON TURNING THROUGH CONSTANT-THICKNESS CIRCULAR-ARC GUIDE VANES IN AXIAL ANNULAR FLOW

By Harry Mankuta and Donald C. Guentert

Lewis Flight Propulsion Laboratory
Cleveland, Ohio

NATIONAL ADVISORY COMMITTEE
FOR AERONAUTICS

WASHINGTON

August 24, 1951

NATIONAL ADVISORY COMMITTEE FOR AERONAUTICS

RESEARCH MEMORANDUM

SOME EFFECTS OF SOLIDITY ON TURNING THROUGH CONSTANT-THICKNESS CIRCULAR-ARC GUIDE VANES IN AXIAL ANNULAR FLOW

By Harry Mankuta and Donald C. Guentert

SUMMARY

An investigation was conducted on sheet metal, circular-arc compressor inlet guide vanes in an annular cascade with untapered walls to determine the effect of solidity on turning through a blade row. Guide vanes of 30° and 40° camber were investigated over a range of solidity from 0.5 to 4.0. The variation in turning with solidity, in the form of a curve of the ratio of turning angle to camber angle plotted against solidity, was compared with similar curves obtained from several two-dimensional methods.

An equation similar in form to Constant's rule, which may be used to predict turning angles in cascades of configuration similar to that of this investigation, was obtained from the data. This equation plotted in the form of turning-angle correction based on a reference solidity may be used to extend the applicability of existing guide-vane data and design rules to other solidities. Because the change in turning angle produced by a change in solidity is probably little affected by blade-thickness distribution and cascade configuration, this turning-angle-correction curve can probably be applied to normal compressor-inlet guide-vane cascade configurations using blades with a circular-arc mean line.

Surveys made downstream of the guide vanes indicated that lower solidities than those presently used (about 1.5) may be employed without exceeding loading limitations (for the inlet Mach number of 0.35 of this investigation).

INTRODUCTION

In order to provide the large inlet flow area required for high weight flows per unit frontal area encountered in high-thrust turbojet engines, the hub-tip ratio at the entrance to the guide vanes is often made equal to 0.5 or less. If the guide vanes are of constant chord, and this is often the case, the solidity at the hub will be as much as double that at the tip. In order to design guide vanes under such conditions, the magnitude of the effect of solidity on the turning angle must be known. Information of this nature is also required where

the number of guide vanes is reduced in an effort to reduce blade costs and weight or to decrease the number of surfaces upon which ice can form in order to minimize heating requirements where inlet-guide-vane de-icing is used. This investigation was conducted to determine experimentally the magnitude of the solidity effect on the turning through circular-arc guide vanes in order to permit the extension of existing data and design rules (for example, reference 1) to other solidities and to compare the experimental turning angles with those predicted by several two-dimensional methods.

Circular-arc guide vanes of 30° and 40° camber with constant chord length were investigated in an untapered annulus over a range of solidity from 0.5 to 4.0, and the results are presented in the form of a ratio of turning angle to camber angle and in terms of a turning-angle correction from a reference solidity. Comparisons of the ratio of turning angle to camber angle are made with the values that would be expected using the turning-angle relation for the turbine cascades of reference 2, the potential flow methods of references 3 and 4, and an equation similar in form to Constant's rule obtained from the data.

Total-pressure surveys were taken downstream of the guide vanes at several radii and are presented in the form of a total-pressure-loss factor for the two blade camber angles investigated in annuli of 10, 20, and 40 blades.

SYMBOLS

The following symbols are used in this report:

a_0 two-dimensional lift slope determined from equations (7) and (8)

c chord length, (in.)

M average angle excess factor

M_1 angle excess factor at inlet, defined by equation (1)

M_2 angle excess factor at outlet, defined by equation (2)

m constant

N number of blades

$\overline{\Delta P_T}$ average total-pressure loss across blade row, (lb/sq ft)

r radius

s distance between corresponding points on two adjacent blades (spacing), (in.)

V_1 upstream velocity, (ft/sec)

α_0 two-dimensional zero-lift angle of attack, determined by equations (7) and (8), (deg)

β_1 angle inlet air makes with perpendicular to cascade axis, (deg)

β_2 angle outlet air makes with perpendicular to cascade axis, (deg)

β_m mean air angle between inlet and outlet air, $\frac{\beta_1 + \beta_2}{2}$, (deg)

γ_1 angle between tangent to blade camber line at the leading edge and the perpendicular to cascade axis, (deg)

γ_2 angle between tangent to blade camber line at the trailing edge and the perpendicular to cascade axis, (deg)

μ angle exaggeration factor, $1/M$

ρ air density, (slugs/cu ft)

θ turning angle, $\beta_2-\beta_1$, (deg)

σ solidity, c/s

φ blade camber angle, (deg)

ζ blade stagger angle, angle between chord and perpendicular to cascade axis, (deg)

ψ singularity exponent, used to determine radial distance of transformed ∞ point to origin of coordinates in unit circle plane, (fig. 7)

$\frac{d\theta}{d\alpha}$ turning angle - angle of attack slope

PROCEDURE AND APPARATUS

Setup. - The apparatus to test the blades consisted of a bellmouth entrance attached to a constant inner- and outer-diameter passage (fig. 1). The constant-chord blades (2.20 in. for 40° camber, 1.67 in. for 30° camber) were made of 1/16-inch sheet metal with tapered

leading and trailing edges and were of constant radius of curvature (3.22 in.). The blades were set with their leading edges tangent to the annulus axis, which resulted in a zero incidence angle with the axially entering air. The upstream Mach number was held constant at 0.35; the Reynolds number based on chord length was constant at 295,000 for 30° camber and 388,000 for 40° camber. Ambient air was taken from the room for the tests and was axial and uniform at the inlet to the guide vanes.

Method of solidity variation. - In order to obtain the required range of solidity between 0.5 and 4.0, initial tests were conducted with 40 blades. These tests provided data within the approximate solidity range of 2.0 to 4.0, which varied with the radius. Data were taken in the solidity range of 1.0 to 2.0 by removing every other blade (leaving only 20 blades); and similarly, data were taken in the solidity range of 0.5 to 1.0 by removing every other blade (leaving only 10 blades). This procedure was followed for two blade camber angles, 30° and 40°.

Measurements. - Instrument surveys were made approximately one chord length upstream and one chord length downstream of the leading edges and trailing edges, respectively. Circumferential instrument surveys for all radii were made downstream over one blade passage to determine the average angle, the static pressure, and the total pressure. Accuracy of the measured turning angle is estimated to be within ±0.5°, the total pressure within ±1 percent of the dynamic pressure, and the static pressure within ±2 percent of the dynamic pressure.

RESULTS AND DISCUSSION

Effect of Solidity on Turning Angle

The turning angles obtained from approximately the middle 60 percent of the flow passage (where end-wall effects were considered small) are shown in figure 2 as the parameter θ/φ plotted against solidity for both cambers investigated. The experimental turning angles used in figure 2 were corrected for axial-velocity changes across the blade row by resolving the velocity diagram to a constant axial velocity equal to the mean of the inlet and outlet axial velocities. The change in solidity from approximately 0.5 to 4.0 covered in this investigation, produced changes in turning angle of about 10° for the 30°-camber blades and about 14° for the 40°-camber blades. Somewhat lower values of θ/φ were obtained with the 40°-camber than with 30°-camber blades; the difference corresponded to approximately 2° at low solidities and approximately 1° at the high solidities.

As described previously, the solidity range of this investigation was covered in three separate tests for each camber angle, using 10, 20, and 40 blades. As a result, three separate groups of data points may be noted in figure 2 corresponding to the three solidity ranges. Although these groups do not match exactly, the differences are considered to be within the accuracy with which the turning angles can be predicted and measured.

Comparison with Two-Dimensional Methods

For comparison with the experimental data, curves of θ/φ obtained from the potential flow methods of references 3 and 4 (described in the appendix) and the rule recommended in reference 2 for turbine-type cascades are presented in figure 2(a). This rule is a modification of Constant's rule and can be expressed as

$$\theta/\varphi = 1 - m\sigma^{-1.0} \tag{1}$$

The value of m for the blade stagger angle of this investigation is approximately 0.2. Good agreement is obtained between the experimental data and the two-dimensional predictions over most of the solidity range. At low solidities, the results of reference 4 give closer agreement with the average data, whereas at higher solidities the results of reference 2 conform more closely with the average data. Values of θ/φ for solidities above 2.5 were not calculated using the method of reference 4 because the method becomes inaccurate at these higher solidities.

The experimental values of θ/φ can be matched fairly well by an equation similar in form to Constant's rule, in which the constants have been modified. The resulting equation may be expressed as

$$\theta/\varphi = 1 - 0.23\ \sigma^{-0.83} \tag{2}$$

A comparison between the experimental values and the values obtained from this equation is shown in figure 2(b).

Application of Results

The curve obtained from equation (2) and plotted in figure 2(b) may be used to predict turning angles (where the end-wall effects are small) in cascades of configuration similar to that of this investigation. Because the turning angle produced by a row of guide vanes will vary with the particular configuration of the cascade (wall taper, blade form, and radial variation of camber), inaccuracies may be

introduced in applying the curve of figure 2(b) to other configurations. However, the change in turning produced by a change in solidity, as indicated by the present results, is expected to be generally applicable to all configurations and blade forms with a circular-arc mean line normally used in guide-vane designs. The turning angles shown in figure 2 are, therefore, plotted in the form of a turning-angle correction factor $\frac{\theta-\theta_{(\sigma=1.6)}}{\varphi}$ to correct the turning angle for changes in solidity. These data are shown in figure 3 and are compared with the values of $\frac{\theta-\theta_{(\sigma=1.6)}}{\varphi}$ obtained from equation (2). It may be noted that the experimental data are somewhat higher at the higher solidities than the values obtained from equation (2). The method used for correcting the turning angles for changes in axial velocity did not account for the influence of solidity on the method of correction. It is probable, however, that the measured turning angle becomes less affected by changes in axial velocity across the blade row as the solidity is increased (that is, as channel flow is approached). For this reason, the experimental data are probably somewhat high at the higher solidities and it is recommended that the curve obtained from equation (2), rather than the experimental points, be used for determining the turning-angle correction factor for changes in solidity.

A reference solidity of 1.6 is used in figure 3 to make the results directly applicable to reference 1, which is based on data the average solidity of which is 1.6. In the present investigation, the change in axial velocity is resolved to a constant axial velocity equal to the mean axial velocity but the method of resolving the change in axial velocity, either to a constant mean axial velocity or a constant inlet axial velocity, was found to have little effect on the experimental values when plotted in the form of the correction factor $\frac{\theta-\theta_{(\sigma=1.6)}}{\varphi}$ of figure 3.

Incidence angles other than zero introduce an additional change in turning angle which is also a function of solidity for a given camber. The turning angle for zero incidence is first calculated using the previously discussed methods and the additional change in turning due to the incidence angle can be applied by the use of figure 4, which is obtained from the potential-flow method of reference 3.

Total-Pressure Losses

Total-pressure surveys were conducted downstream of the blades at several radii and are plotted in figure 5 in the form of a

total-pressure-loss factor $\frac{\overline{\Delta P_T}}{\frac{1}{2}\rho V_1^2}$ for the two blade camber angles investigated where $\overline{\Delta P_T}$ is the arithmetic average of the total-pressure loss in one blade passage at a given radius. In the middle portion of the blade height, where the end effects are small, the total-pressure loss, in general, decreases with decreasing solidity or number of blades until a minimum solidity is reached, at which point the blade loading will become excessive and separation will occur causing considerable increase in the total-pressure losses. Evidence that such excessive blade loading has occurred beyond the radius of 4.66 for the 40° camber blades ($N = 10$) is provided by the sharp increase of $\frac{\overline{\Delta P_T}}{\frac{1}{2}\rho V_1^2}$ with radius. The solidity at the radius of 4.66 was 0.75 and the lift coefficient for the inlet Mach number of these tests of 0.35 was calculated to be 1.4.

Although lowering the solidity may decrease the total-pressure losses, increases in circumferential flow variations that may accompany a decrease in the number of guide vanes and that may adversely affect the performance of subsequent blade rows must also be considered when reducing the number of guide vanes. Although setting a lower limit on the solidity of constant-thickness, circular-arc guide vanes is impossible, as this limit will vary with the particular application, it appears that they may be designed with lower solidities than are commonly used (about 1.5) and still not introduce serious circumferential flow variations. These lower solidities may be advantageous where it is desired to reduce the blade costs and weight or to decrease the surfaces upon which ice can form in order to minimize heating requirements where inlet-guide-vane de-icing is used.

CONCLUDING REMARKS

The results of this investigation to determine the effect of solidity on turning through a blade row indicate that the equation $\theta/\varphi = 1 - 0.23\,\sigma^{-0.83}$, where θ is turning angle, φ is blade camber angle, and σ is solidity, can be used with reasonable accuracy in the blade-height portion unaffected by the end walls for predicting the turning angle through guide-vane cascades with configurations similar to that of this investigation.

This equation plotted in the form of a turning-angle correction based on a reference solidity may be used to extend the applicability of existing guide-vane data and design rules to other solidities.

Because the change in turning angle produced by a change in solidity is probably little affected by blade-thickness distribution and cascade configuration, this turning-angle-correction curve can probably be applied to any normal inlet-guide-vane cascade configuration using blades with a circular-arc mean line.

For an inlet Mach number of 0.35, indications are that solidities lower than those currently used may be employed in compressor inlet-guide-vane designs without exceeding loading limitations.

Lewis Flight Propulsion Laboratory,
National Advisory Committee for Aeronautics,
Cleveland, Ohio.

APPENDIX - POTENTIAL FLOW THROUGH CASCADE OF CIRCULAR ARCS

The potential-flow theory of the methods herein referred to is applicable to a general circular-arc cascade at any incidence angle. In order to make the theoretical methods comparable to the present investigation, the blade orientation must be so adjusted that the leading edge is perpendicular to the cascade axis and the inlet-air angle is tangent to the leading edge.

Method of reference 3. - According to the method of reference 3, smooth through flow in a cascade of circular-arc blades requires that the angle excess at the leading and the trailing edge be equal, where the angle excess is defined as the difference between the air angle and the tangent to the circular arc at the leading or trailing edge. Under these conditions, $M_1 = M_2 = M$ where

$$M_1 = \frac{\beta_m - \gamma_1}{\beta_m - \beta_1} \tag{A1}$$

$$M_2 = \frac{\beta_m - \gamma_2}{\beta_m - \beta_2} \tag{A2}$$

Solving for the inlet- and outlet-air angles for the condition where the tangent to the leading edge is perpendicular to the cascade direction, that is, $\gamma_1 = 0$ yields

$$\beta_1 = \frac{2\gamma_2 (M-1)}{(M+1)^2 - (M-1)^2} \tag{A3}$$

and

$$\beta_2 = \frac{2\gamma_2 (M+1)}{(M+1)^2 - (M-1)^2} \tag{A4}$$

where γ_2 coincides with the camber angle and M may be obtained as the reciprocal of the turning-angle exaggeration factor μ, given as a function of solidity and mean air angle $\beta_m = \zeta$ in figure 6. By use of the preceding equations, the inlet- and outlet-air angles can be determined for smooth through flow for a cascade of given solidity and camber. Because a zero incidence angle is desired, the inlet-air angle must be changed by an amount equal to β_1. The effect of this

change on β_2 may be determined from figure 4, which was obtained by the use of the methods of reference 3 and gives the theoretical change in turning angle for small changes in angle of attack over a range of solidities. Thus, the outlet-air angle β_2 can be determined for a cascade of circular blades of given camber and solidity set at zero incidence.

Method of reference 4. - This method, which is based on the concept of the thin airfoil, was developed for application to decelerating flow. It does not lend itself to predicting the local flow distribution near the airfoils, but at a slight distance downstream of the trailing edges the flow field is very close to that of the real airfoil. Inasmuch as the air-outlet direction is the primary concern of this report and not the distribution of the air forces on the blades, this method should be sufficiently accurate.

The relation between outlet- and inlet-air angle is given in appendix III of reference 4 for a decelerating cascade as

$$\tan \beta_2 = \frac{\frac{c}{2s} a_0 \sin (\zeta-\alpha_0) + \tan \beta_1 \left[1 - \frac{c}{4s} a_0 \cos (\zeta-\alpha_0)\right]}{1 + \frac{c}{4s} a_0 \cos (\zeta-\alpha_0)} \tag{A5}$$

For accelerating flow this equation becomes

$$\tan \beta_2 = \frac{\frac{c}{2s} a_0 \sin (\zeta+\alpha_0) + \tan \beta_1 \left[1 - \frac{c}{4s} a_0 \cos (\zeta+\alpha_0)\right]}{1 + \frac{c}{4s} a_0 \cos (\zeta+\alpha_0)} \tag{A6}$$

where

$$a_0 \sin \alpha_0 = \frac{8}{\pi} \left(\frac{s}{c}\right)^2 \tan \frac{\varphi}{2} \ln (\coth \psi) \tag{A7}$$

$$a_0 \cos \alpha_0 = 4 \left(\frac{s}{c}\right) \frac{\sqrt{2}}{\sqrt{\cosh 2\psi + \cos 2\zeta}} \tag{A8}$$

Values of ψ plotted against s/c are shown in figure 7.

Because the slopes of the curves of turning angle against blade camber angle are practically constant for any given solidity, a single curve of θ/φ against solidity (fig. 2) can be obtained. Comparisons of the results of the two methods showed that good agreement was obtained in the outlet-air angles predicted by the two methods at a solidity of about 1.5. Below this solidity, the method of reference 4

appeared to give results more in agreement with the data, whereas at solidities above 1.5, the method of reference 3 appeared better.

REFERENCES

1. Lieblein, Seymour: Turning-Angle Design Rules for Constant-Thickness Circular-Arc Inlet Guide Vanes in Axial Annular Flow. NACA TN 2179, 1950.

2. Carter, A. D. S.: The Low Speed Performance of Related Airfoils in Cascade. Rep. No. R.55, British N.G.T.E., Sept., 1949.

3. Weinig, F.: The Flow around Turbine and Compressor Blades. CGD 291, reproduced by Code 338, Res. and Standards Branch. BuShips, Navy Dept., May 1946. (Abs. Bib. Sci. Ind. vol. 2, no. 13, April 5, 1946, p. 997, PB 28689.)

4. Bowen, John T., Sabersky, Rolf H., and Rannie, W. Duncan: Theoretical and Experimental Investigations of Axial Flow Compressors. Mech. Eng. Lab., C.I.T., Jan. 1949. (Navy Contract N6-ORI-102, Task Order IV).

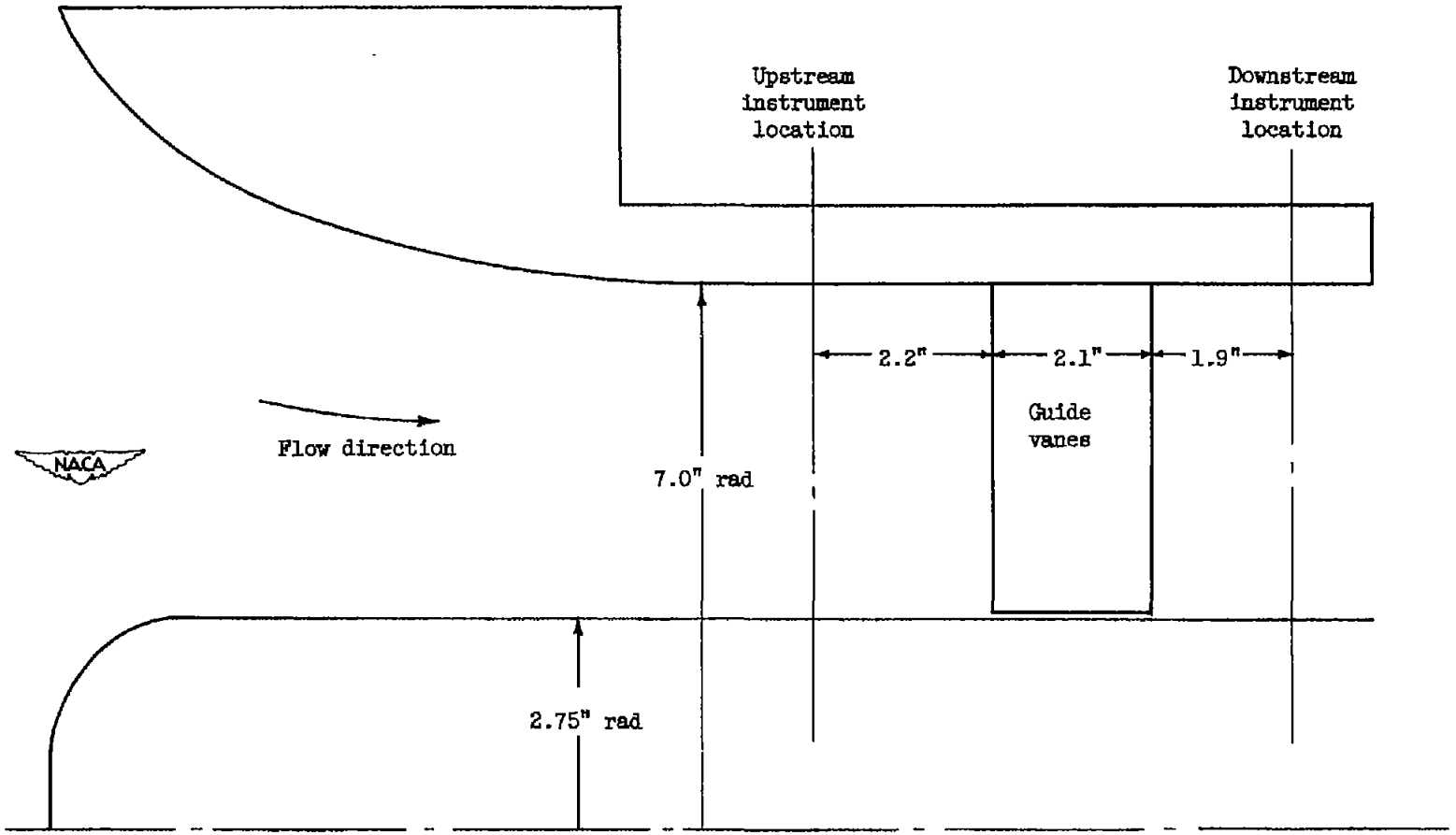

Figure 1. - Cross-sectional view of test annulus and location of survey instruments.

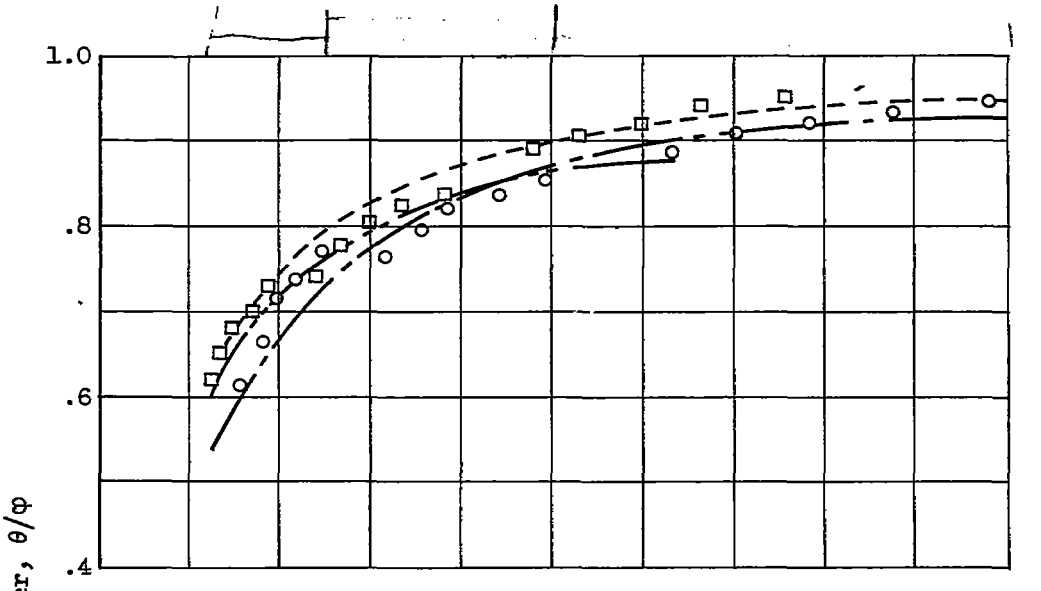

(a) Two-dimensional methods.

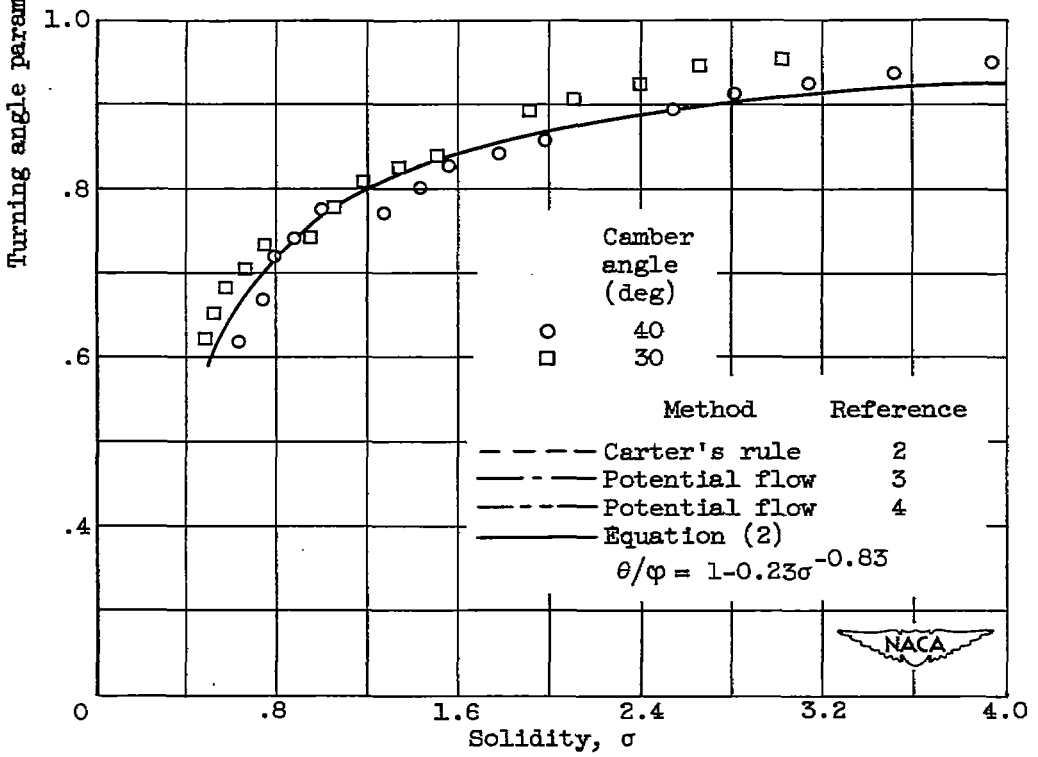

(b) Equation (2).

Figure 2. - Comparison of experimental turning angles for 30° and 40° cambered constant-thickness, constant-chord, circular-arc guide vanes in nontapered annuli with turning angles predicted by other methods.

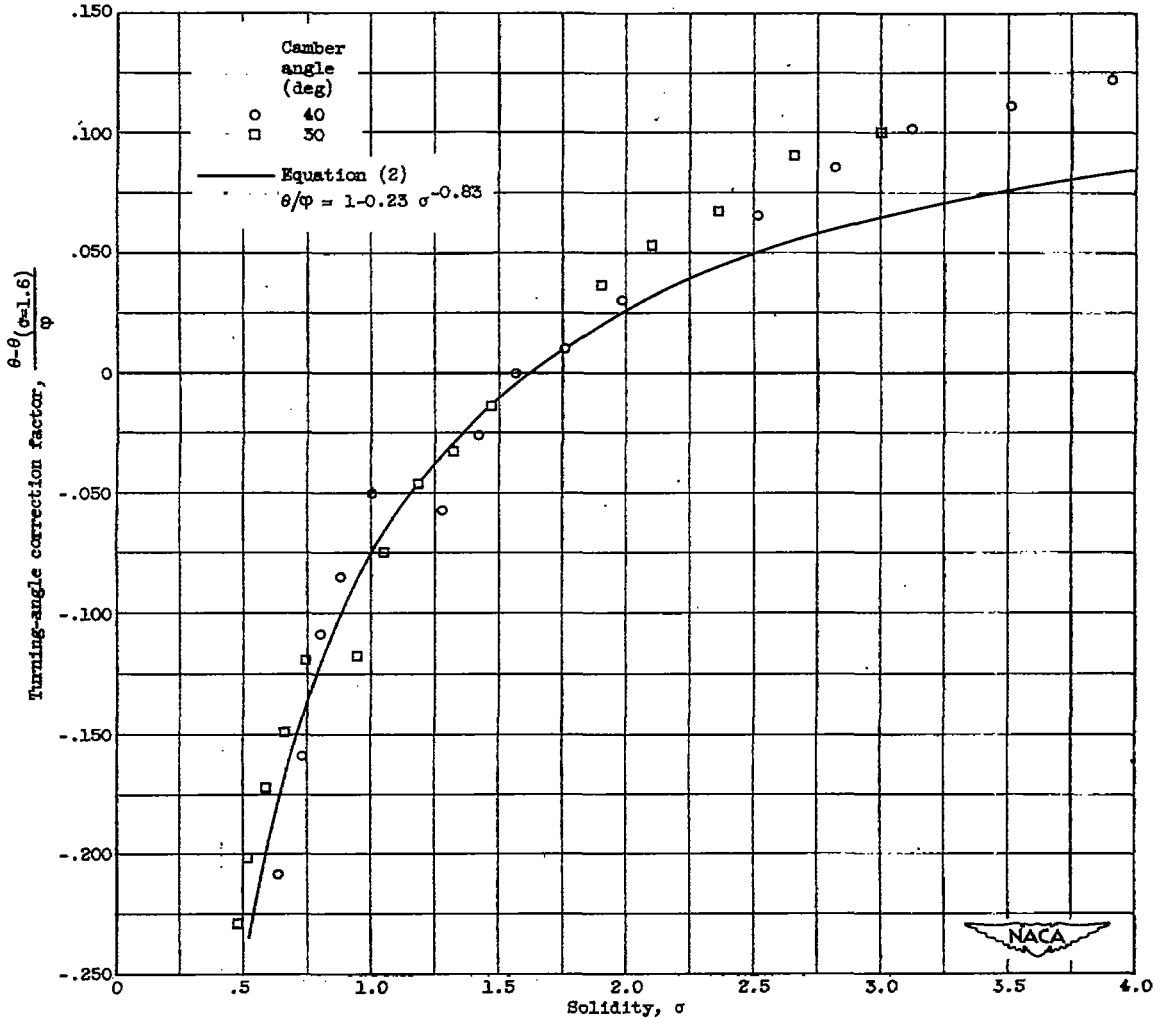

Figure 5. - Variation of turning-angle correction factor with solidity.

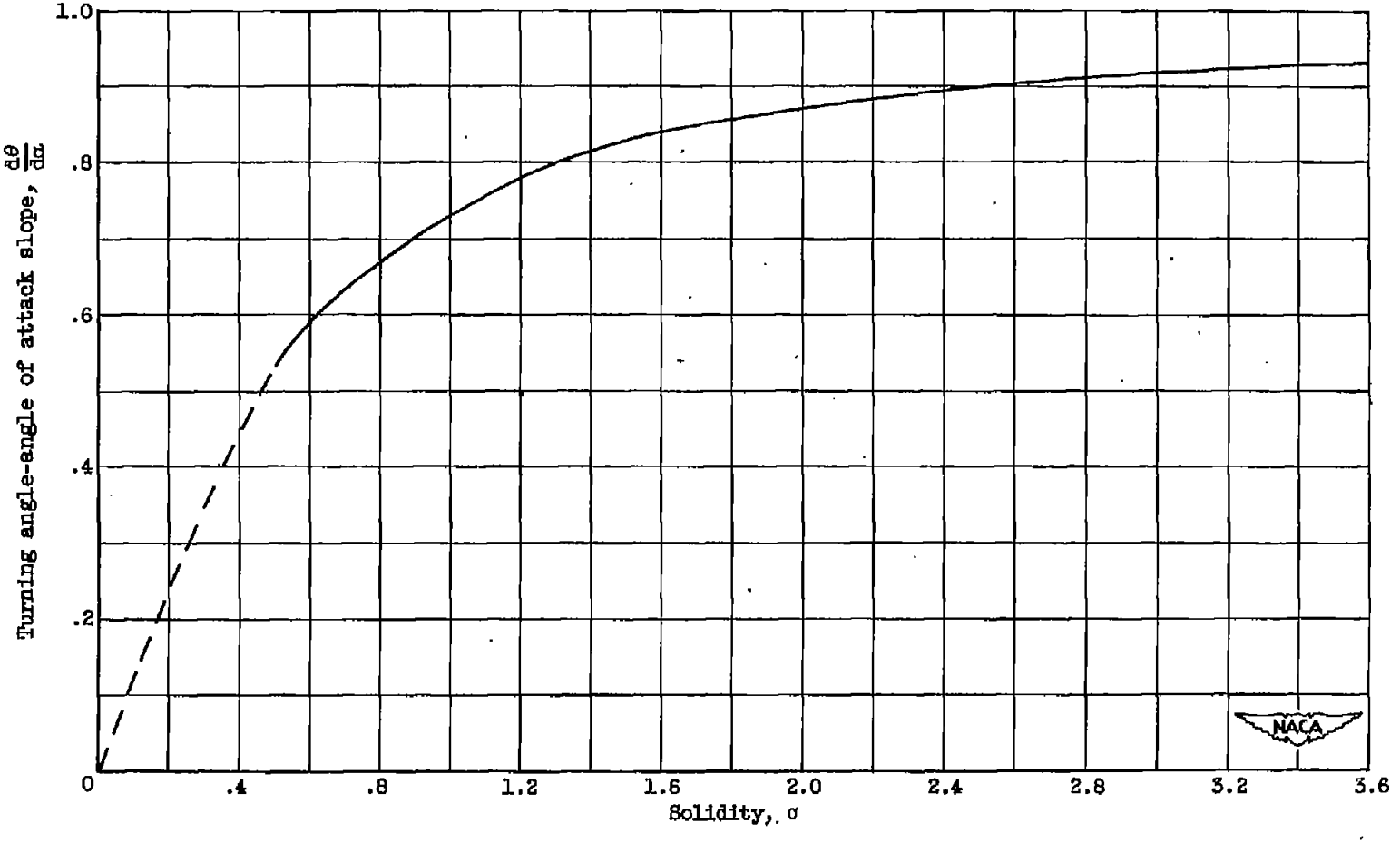

Figure 4. - Potential-flow two-dimensional turning angle - angle of attack slope for accelerating cascades at zero incidence, zero stagger angle.

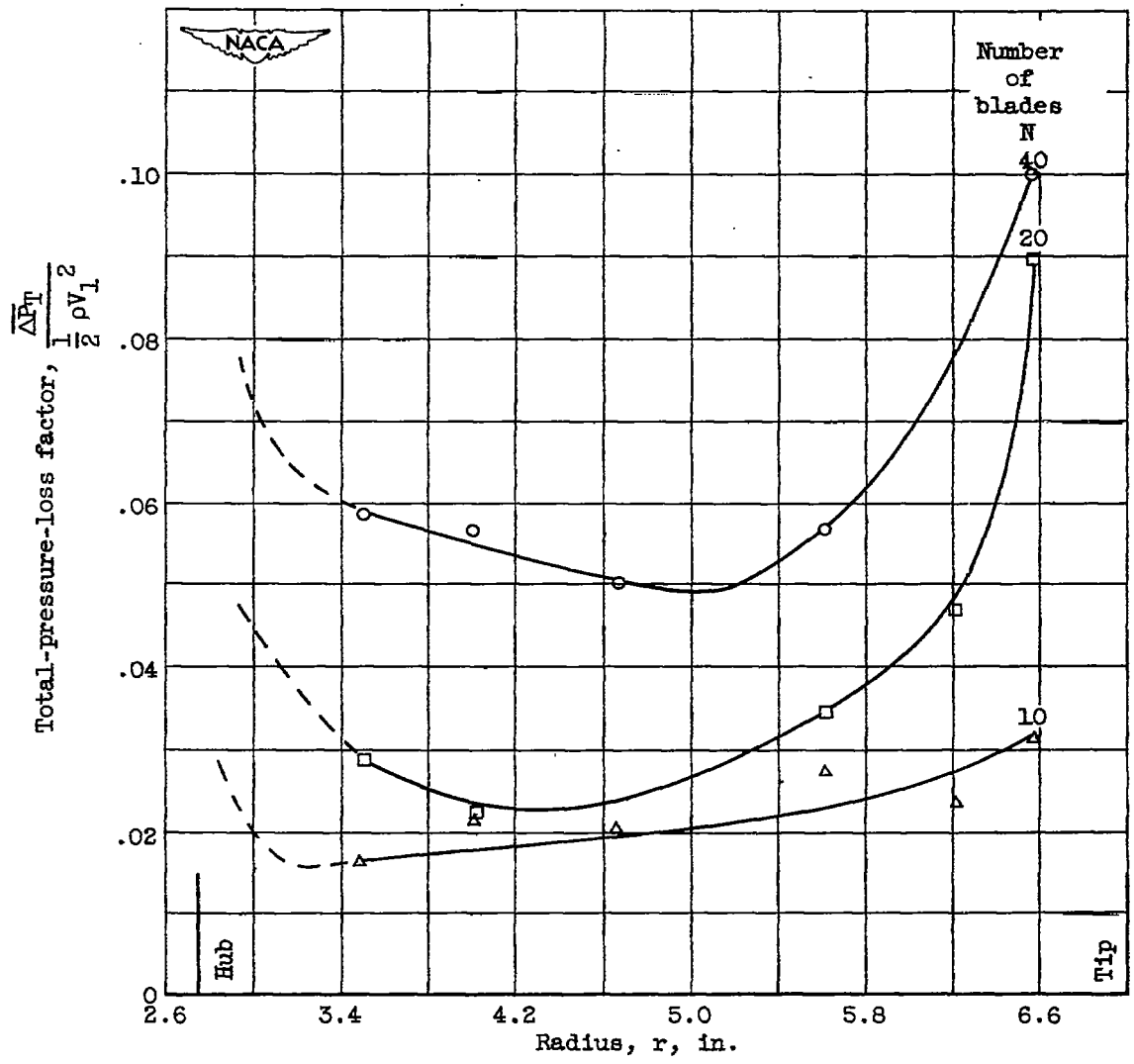

(a) Camber angle, 30°.

Figure 5. - Variation of total-pressure losses through annular cascade of constant-thickness, circular-arc guide vanes.

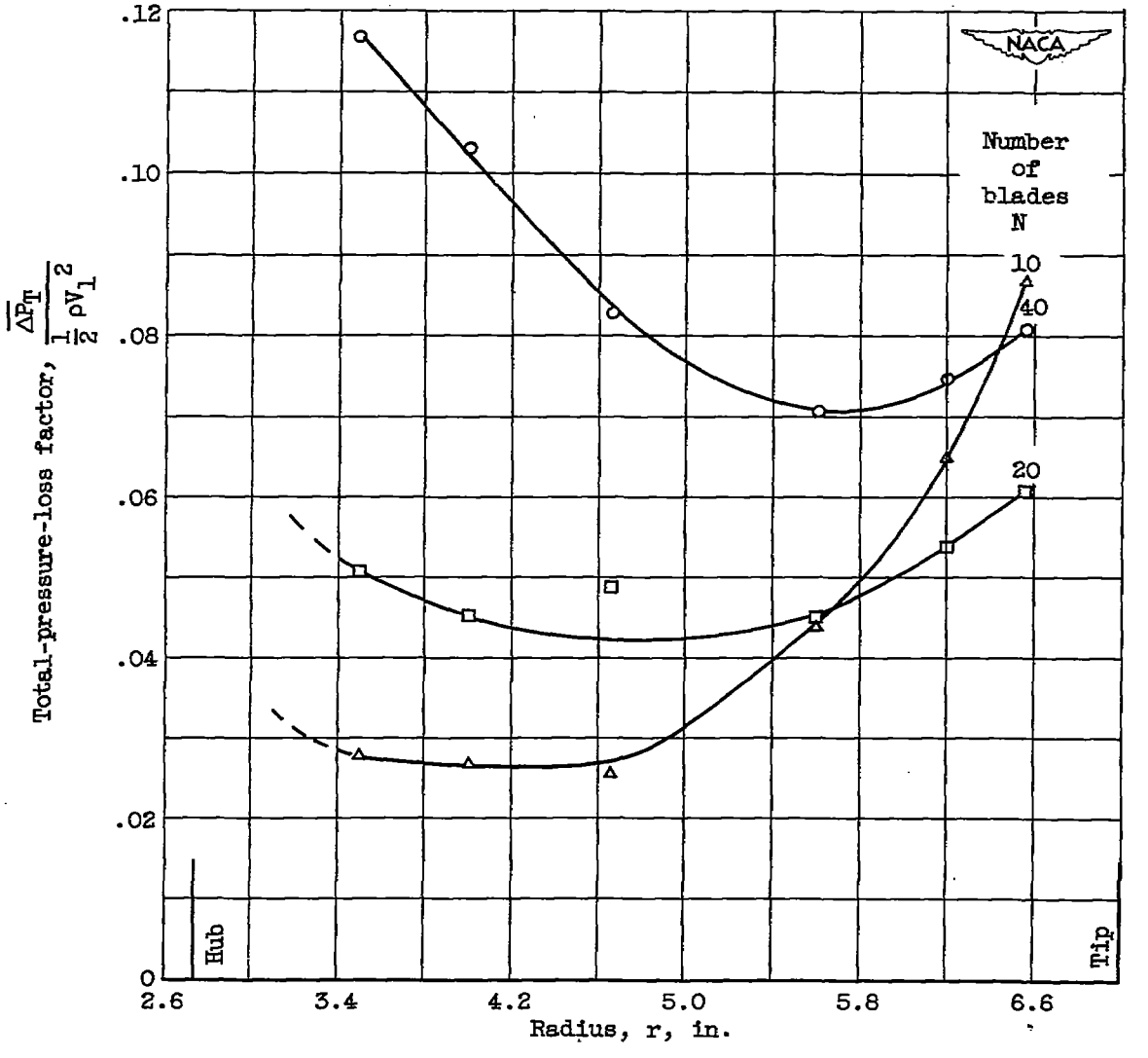

(b) Camber angle, 40°.

Figure 5. - Concluded. Variation of total-pressure losses through annular cascade of constant-thickness, circular-arc guide vanes.

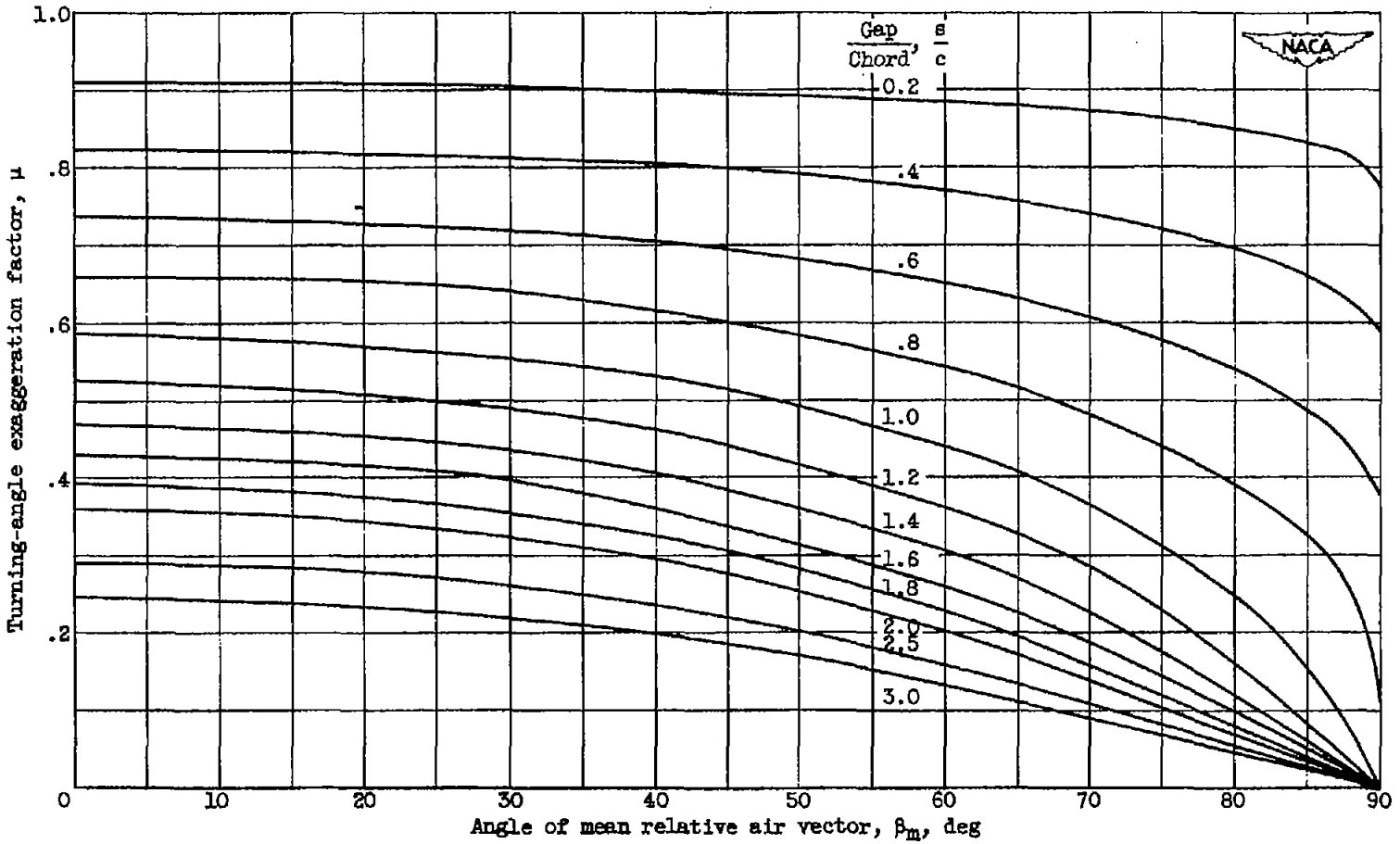

Figure 6. - Variation of turning-angle exaggeration factor with mean relative air vector for various gap-chord ratios. (Fig. 81 of reference 3.)

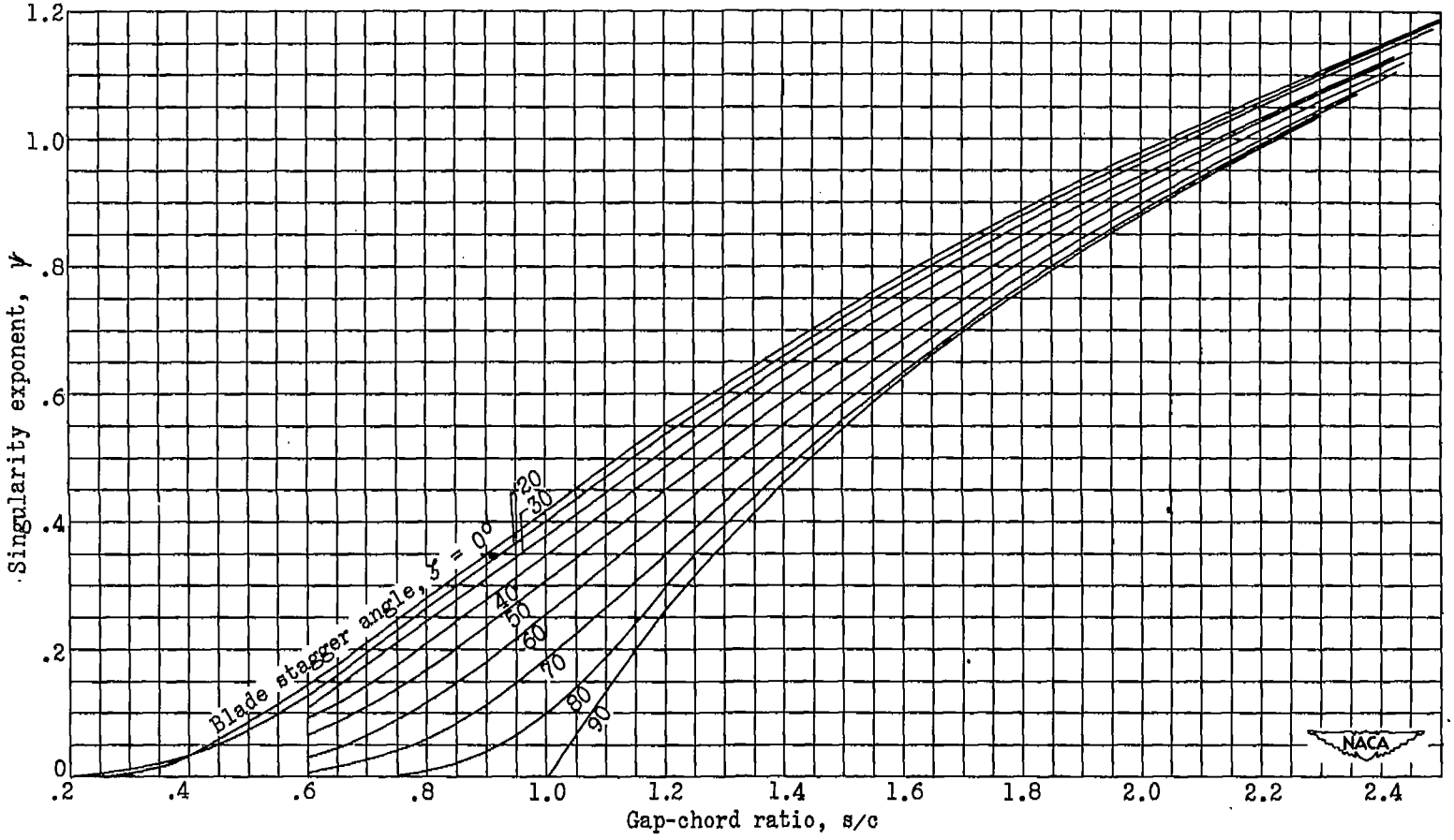

Figure 7. - Variation of singularity exponent with gap-chord ratio for various blade stagger angles. (Fig. 82 of reference 4.)